

Label-free proteomic analysis and functional analysis in patients with intrauterine adhesion

Jingxuan Ye¹, Yong Li^{1,*}, Chengcai Kong¹, Yiwen Ren¹, Hangcheng Lu¹

Changzhou maternal and Child Health Care Hospital, Changzhou Medical Center, Nanjing Medical University, China



ARTICLE INFO

Keywords:

Intrauterine adhesion
Endometrium
Label-free proteomics
Parallel reaction monitoring
Fibrosis

ABSTRACT

Intrauterine adhesion (IUA) is one of the principal causes of secondary infertility in women of reproductive age, which seriously affects female reproductive function and quality of life. In recent years, the incidence of IUA has been increasing year by year, but its pathological mechanism has not yet been clarified. This study intended to reveal the pathogenesis of IUA and find new therapeutic targets by analyzing the proteomic differences between intrauterine adhesion tissues and normal human endometrial tissues. In the label-free quantitative proteomics, we identified 789 up-regulated differentially expressed proteins (DEPs) and 539 down-regulated DEPs. These DEPs were further analyzed by Gene Ontology (GO) annotation and enrichment analysis, Kyoto encyclopedia of genes and genomes (KEGG) enrichment analysis to preliminarily clarify the biomarkers involved in the pathogenesis of the IUA. The DEPs were further verified by parallel reaction monitoring (PRM) to confirm the results of proteomics. Finally, 7 target proteins may be candidates for treatment and elucidating the pathophysiology of IUA.

Significance: IUA is a fertility complication, which has increasing incidence recently. Until now, only a little research paid attention to the proteomic changes of IUA. This is the first study focused on the comparative analysis of endometrial tissue between IUA patients and normal women. We found 7 key proteins that may become the potential biomarkers of IUA.

1. Introduction

Intrauterine adhesion (IUA), also called Asherman's syndrome, refers to the trauma of the endometrial basal layer which causes tissue adhesions of the uterine cavity [1]. The main clinical manifestations of IUA are characterized by decreased menstrual flow or even amenorrhea, recurrent miscarriage, and secondary infertility [2]. The primary pathological damage from IUA is endometrial fibrosis caused by the massive deposition of extracellular matrix [3]. However, the pathogenesis of IUA remains unclear. The current mainstream treatment cannot fundamentally prevent endometrial fibrosis, and hysteroscopic surgery may further damage the endometrium. The recurrence rate of moderate to severe IUA is as high as 60% or more [4]. Therefore, it is crucial to identify the molecular therapeutic targets of IUA.

IUA is closely related to the abnormal expression of pro-fibrotic proteins such as transforming growth factor-beta1 (TGF- β 1). After the endometrial injury, the increased expression of TGF- β 1 stimulated the overexpression of the downstream connective tissue growth factor

(CTGF) and inhibited the activity of matrix metalloproteinase-9 (MMP-9), and led to the massive deposition of extracellular matrix as well as the occurrence of endometrial fibrosis [5,6]. Totally, Proteomics can identify biomarkers of various diseases and combine mass spectrometry with biological information to detect the occurrence and development of the disease [7]. Subsequently, through relevant verification, the key markers or therapeutic targets would be selected from all the DEPs.

In this research, we carried out a label-free quantitative proteomic analysis between human IUA tissue and normal endometrial tissue. Throughout detailed bioinformatics analysis of DEPs, we found that they are involved in cellular processes, biological regulation, protein other processes, and various signaling pathways including focal adhesion and actin cytoskeleton regulation. To obtain more comprehensive changes in the DEPs in IUA patients, 7 target proteins were identified (PGM5, CAMK2G, ABHD6, MYLK, SYNPO2, IRAG1, ADIPOQ) through parallel reaction monitoring. These target proteins maybe provide the directive discovery of IUA targets in the future.

* Corresponding author.

E-mail address: liyisheng2013@qq.com (Y. Li).

¹ Full postal address: No. 16, Dingxiang Road, Zhonglou District, Changzhou City, Jiangsu Province.

2. Materials and method

2.1. Sample collection

Prior to commencing the study, ethical clearance was sought from the Ethics Committee of Changzhou Maternal and Child Health Hospital. All patients signed informed consent. The intrauterine adhesion tissues of five patients with IUA confirmed by hysteroscopy or pathological examination were collected, and the endometrial tissues of the patients with uterine fibroids (except for submucosal fibroids) were obtained as the normal endometrial control groups. Because the existence of intra-mural or subserosal fibroids will not influence the endometrium like diseases such as hydrosalpinx and uterine septum. All tissue specimens were collected 3 to 7 days after menstruation. None of the patients took estrogen and progesterone within 6 months before sampling and none experienced other medical and surgical complications, or intrauterine infection. Demographic information, including age, body mass index (BMI), and preoperative hemoglobin (HG) level, were recorded. The collected specimens were stored at -80 °C freezer for subsequent proteomic analysis.

2.2. Protein extraction and trypsin digestion

An appropriate amount of cryopreserved tissue was weighed and ground to a powder, then the resultant tissues were transferred to a centrifuge tube and resuspended in four volumes of lysis buffer (1% Triton X-100, 1% protease inhibitor cocktail). Centrifuging at 12,000g for 10 min at 4 °C to remove the debris remaining after they were sonicated by a high-intensity sonicator. The protein concentration of the supernatant was determined using the BCA kit (Beyotime, China).

Take an equal amount of 300 µg protein for enzymatic hydrolysis of each sample. Add TCA (Trichloroacetic acid, Sigma-Aldrich) at a final concentration of 20% and precipitate the samples at 4 °C for 2 h. After centrifuged at 4500 × g for 5 min, the supernatant was discarded, then wash the pellet 2–3 times with acetone and dry them. Add TEAB (Tetraethylammonium bromide, Sigma-Aldrich) to a final concentration of 200 mM. After ultrasonically dispersing the precipitate, trypsin was added at a ratio of 1:50 (protease: protein, m/m) for overnight enzymatic digestion. Add dithiothreitol (DTT) to make precipitation at a final concentration of 5 mM and reduce 30 min at 56 °C. Then, iodoacetamide (IAA) was added to make the final concentration 11 mM and incubated at room temperature for 15 min in the dark.

2.3. LC-MS/MS analysis

The tryptic peptides were dissolved in solvent A (0.1% formic acid, 2% acetonitrile/ in water), and directly loaded onto a home-made reversed-phase analytical column (25-cm length, 100 µm i.d.). Peptides were separated with a gradient from 3% to 10% solvent B (0.1% formic acid in 90% acetonitrile) over 3 min, 10% to 23% in 67 min, 23% to 33% in 13 min, and climbing to 80% in 4 min then holding at 80% for the last 3 min, all at a constant flowrate of 450 nL/min on an UltiMate 3000 UPLC system (Thermo Fisher Scientific). The separated peptides were analyzed in Orbitrap Exploris 480 (Thermo Fisher Scientific) with a nano-electrospray ion source. The electrospray voltage applied was 2.0 kV. The full MS scan resolution was set to 60,000 for a scan range of 400–1200 *m/z*. Up to 25 most abundant precursors were then selected for further MS/MS analyses with 30 s dynamic exclusion. The HCD fragmentation was performed at a normalized collision energy (NCE) of 27%. The fragments were detected in the Orbitrap at a resolution of 15,000. Fixed first mass was set as 110 *m/z*. Automatic gain control (AGC) target was set at 100%, with an intensity threshold of 5e4 and a maximum injection time of auto.

2.4. Data analysis

The resulting MS/MS data were processed using Proteome Discoverer (v2.4.1.15) search engine with the Sequest. Tandem mass spectra were searched against the human SwissProt database (20,387 entries) concatenated with reverse decoy database. Trypsin/P was specified as cleavage enzyme allowing up to 2 missing cleavages. The mass tolerance for precursor ions was set as 20 ppm in First search and 5 ppm in Main search, and the mass tolerance for fragment ions was set as 0.02 Da. Carbamidomethyl on Cys was specified as fixed modification. Acetylation on protein N-terminal, oxidation on Met and deamidation (NQ) were specified as variable modifications. FDR was adjusted to <1% and minimum score for peptides was set >40. Differential analysis was performed to identify proteins by repeatability test.

2.5. Protein annotation

Using eggnoG-mapper software (v2.0) to perform Gene Ontology (GO) annotation analysis of the DEPs. The software extracted the GO ID of each protein annotation result and classified the proteins according to their cellular components, molecular functions, and biological processes. Using the Pfam database and the corresponding PfamScan tool to perform protein domain annotation of the identified proteins. Protein pathways were annotated based on the KEGG pathway database and the identified proteins were performed BLAST alignment (blastp, e value ≤1e4). Each sequence was conducted with BLAST alignment and the result with the highest alignment score was recorded.

2.6. Protein functional enrichment

Based on the identified proteins, using fisher's exact test to perform GO enrichment analysis, KEGG enrichment analysis and domain enrichment analysis of the DEPs. *P*-value <0.05 was considered as significant.

2.7. Parallel reaction monitoring

Differential abundance of selected proteins was verified using PRM quantitative analysis. The sample was fractionated into fractions by high pH reverse-phase HPLC using Agilent 300Extend C18 column (5 µm particles, 4.6 mm ID, 250 mm length), and wavelength was set to 214 nm, the column oven temperature was set to 35 °C, used 95% buffer A (2% ACN, pH 9.0 adjusted by ammonia) and 5% buffer B (98% ACN, pH 9.0 adjusted by ammonia) equilibrated the column for 30 min at least. Sent the stepwise gradient method after the baseline became flat. Then, add 1 mL buffer A to the peptide sample and vortex to dissolve it. Centrifuge the sample at 12000 g for 5 min and transfer it to a new tube. Centrifuge it again to take the supernatant and load the sample to the HPLC, send the method to separate the sample, and at the same time start the automatic collector. Collect the sample at 1 min/tube and from the 11th to 46th tubes total of 36 tubes. At the last, the peptides were combined into 4 fractions and dried by vacuum centrifuging.

The tryptic peptides were dissolved in 0.1% formic acid (solvent A), and directly loaded onto a homemade reversed-phase analytical column (25-cm length, 100 µm i.d.). The gradient was comprised of an increase from 6% to 20% solvent B (0.1% formic acid in 98% acetonitrile) over 16 min, 20% to 30% in 6 min and climbing to 80% in 4 min then holding at 80% for the last 4 min, all at a constant flow rate of 500 nL/min on an EASY-nLC 1000 UPLC system.

The peptides were subjected to NSI source followed by tandem mass spectrometry (MS/MS) in Q ExactiveTM Plus (Thermo) coupled online to the UPLC. The electrospray voltage applied was 2.0 kV. The *m/z* scan range was 398 to 1045 for the full scan, and intact peptides were detected in the Orbitrap at a resolution of 60,000. Peptides were then selected for MS/MS using the NCE setting as 27 and the fragments were detected in the Orbitrap at a resolution of 15,000. The PRM method used

Table 1
Informations of the recruited patients.

IUA Tissue Group	Control Group	P-Value
Age (year) (mean \pm SD)	29.60 \pm 3.44	32.60 \pm 2.88
BMI (kg/m ²) (median(IQR))	20.83(3.35)	23.44(2.37)
HB(g/L)(mean \pm SD)	133.00 \pm 8.80	129.80 \pm 8.08

SD, standard deviation. BMI, body mass index. IQR, interquartile range. HB, hemoglobin.

in our research include MS full scan and DIA acquisition combined with a target list, this method can achieve the same effect as PRM. So the data acquisition mode used DIA method with the HCD fragmentation setting to 27. The DIA setup method was the target peptide mass-to-charge ratio. Automatic gain control (AGC) was set at 3e6 for full MS and 1e5 for MS/MS. The maximum IT was set at 200 ms for full MS and auto for MS/MS. The isolation window for MS/MS was set at 1.6 m/z.

Using Maxquant (v1.6.15.0) to retrieve secondary mass spectrometry data [8]. The resulting MS data were processed using Skyline (v.21.1). The peptide parameters were as follows: set the protease to Trypsin[KR/P] and the maximum number of missed cleavage sites to 0. Peptides are 7–25 amino acid residues in length. Variable modification was set as Carbamidomethyl on Cys and oxidation on Met, and max variable modifications were set as 3. Transition parameters: set the parent ion charge to 2, 3, set the production charge to 1, and the ion type was set to b, y. Fragment ions are picked from 3 to last, and the mass error tolerance for ion matching was set to 0.02 Da. The proteins with $p < 0.05$ were considered significantly differentially expressed.

Our experiment was completed in Jingjie PTM BioLab (Hangzhou) Co. Ltd.

2.8. Statistical analysis

The Shapiro-Wilk test was used to evaluate the normal distribution of

continuous variables. When continuous variables satisfied a normal distribution, they were expressed as the mean \pm standard deviation, otherwise, the median was expressed by the interquartile range (IQR). Comparisons of continuous variables between the two groups were performed using the t-test or the Mann-Whitney U test, depending on whether the variables were normally distributed. Fisher's exact test was used to detect DEPs. A p -value less than 0.05 was considered statistically significant. Differential analysis was performed by Pearson's repeatability test to identify proteins. When the P -value < 0.05 , the change of one DEP was greater than 1.5 as the change threshold for significant up-regulation, and less than 1/1.5 for significant down-regulation. All analyses were carried out using SPSS, version 25.

3. Result

3.1. Sample features

Our study recruited 5 IUA patients and 5 patients with uterine fibroids as control groups. The average ages of the two groups were 29.60 \pm 3.44 years and 32.60 \pm 2.88 years, with no significant difference ($P = 0.557$) (Table 1). Both the mean BMI and preoperative HB values were also not significantly different between the two groups ($P > 0.05$) (Table 1).

3.2. Differentially expressed proteins between intrauterine adhesions and normal endometrium

We analyzed the samples of intrauterine adhesions and normal endometrium (including 5 IUA tissues and 5 normal endometrial tissues) using label-free quantitative proteomics. When the $P < 0.05$, the protein expression of the IUA group was 1.5-fold higher than that of the control group or lower than that of the control group (≤ 0.67 -fold) were considered to be DEPs. A total of 1328 differential expressed proteins were identified, of which 789 proteins were up-regulated and 539

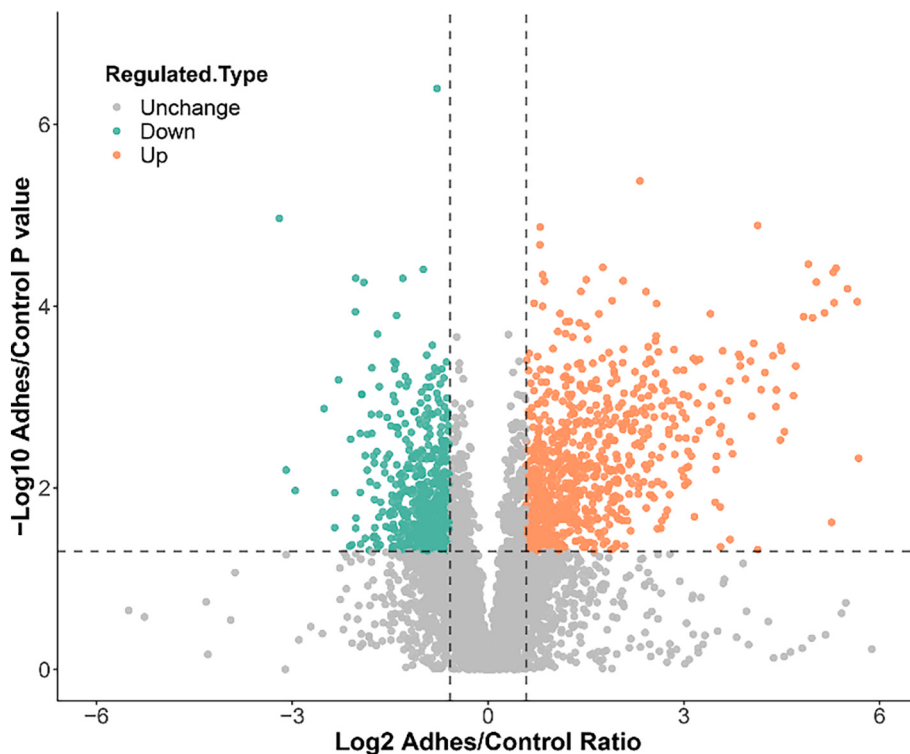
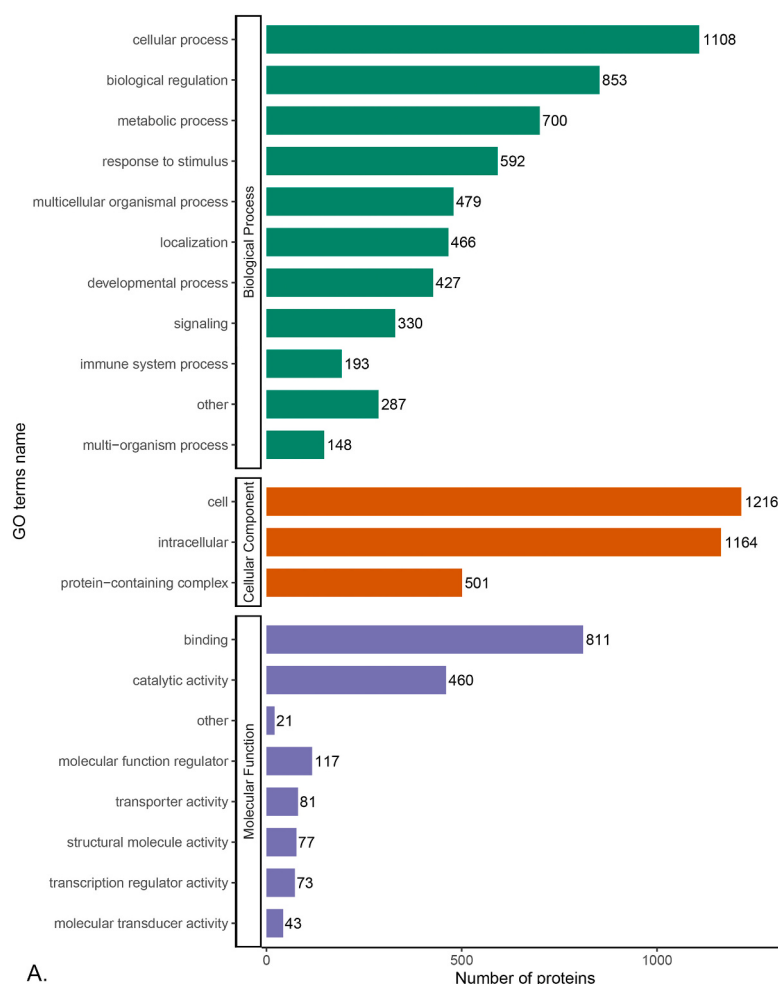
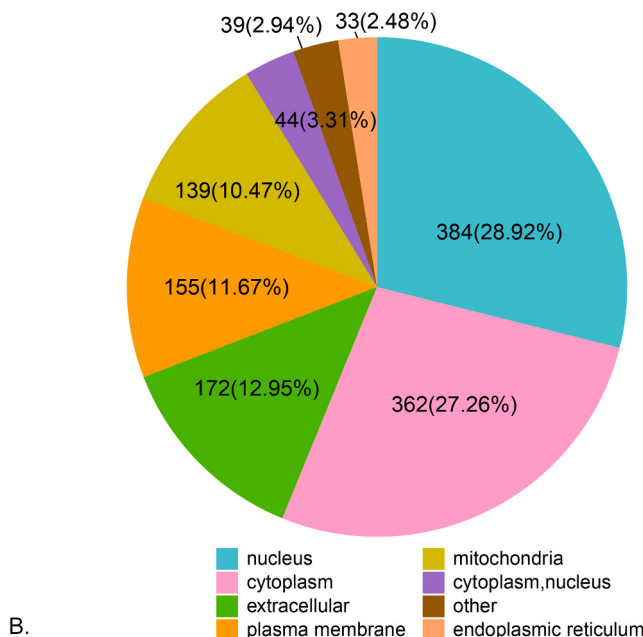


Fig. 1. The volcano plot showed the DEPs between the intrauterine adhesion group and the control group. Up-regulated proteins ($n = 789$) were labeled in red, and the green dots on the left represented down-regulated proteins ($n = 539$). The gray dots represented proteins with no significant differences. (For interpretation of the references to color in this figure legend, the reader is referred to the web version of this article.)

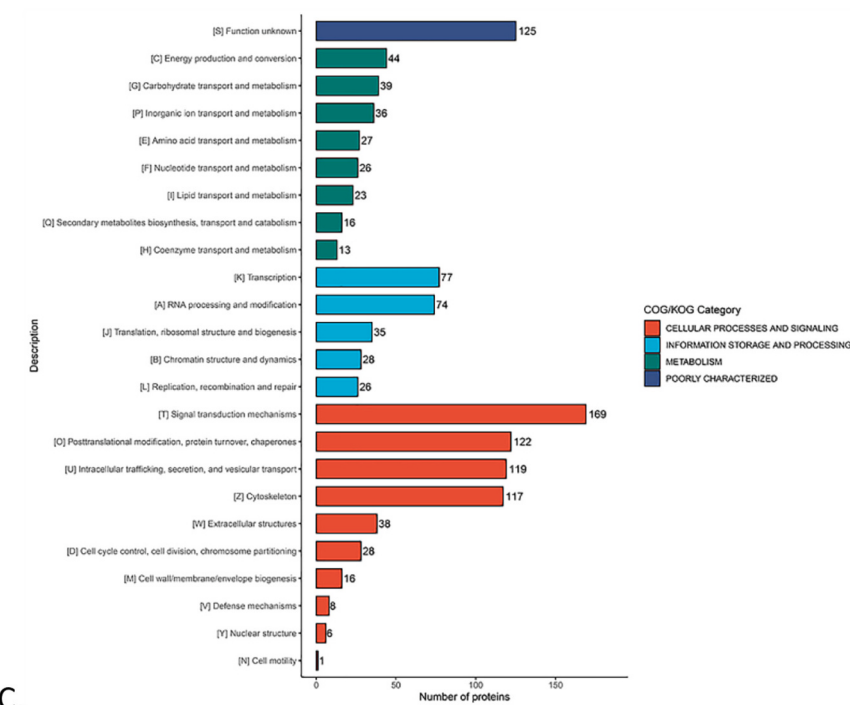


A.



B.

Fig. 2. GO annotation, subcellular localization analysis and COG/KOG functional classification of the DEPs. A, The GO annotation of the DEPs. B, Subcellular localization of the DEPs. C, COG/KOG functional classification of the DEPs.



C.

Fig. 2. (continued).

proteins were down-regulated. The volcano map of the DEPs is shown in Fig. 1.

3.3. The functional analysis of the DEPs

3.3.1. GO annotation and COG/KOG functional classification

GO annotations, including biological processes, molecular functions and cellular components, annotates the biological roles of proteins from different perspectives [9]. Our results showed that the IUA-related DEPs are mainly involved in biological processes such as cellular processes, biological regulation, and metabolism processes. They mainly played a role in molecular functions such as binding, catalytic activity and molecular function regulator. (Fig. 2A) Subcellular localization analysis indicated that 28.92% of the DEPs were localized in the nucleus and 27.26% of the DEPs were localized in the cytoplasm (27.26%) (Fig. 2B). According to the results of the COG/KOG functional classification, the DEPs were mainly related to signal transduction mechanisms and post-translational modification, protein turnover, chaperones (Fig. 2C).

3.3.2. Enrichment analysis

3.3.2.1. GO enrichment analysis. GO enrichment analysis of the DEPs was performed between the two groups to determine the significant enrichment trend of the DEPs. We drew a bubble chart and gave the results of the top 20 most clearly enriched categories top, and the results showed that the biological process of the up-regulated proteins was significantly enriched in the regulation of ion transport, cell junction assembly, and regulation of muscle system process (Fig. 3A). The biological processes of the downregulated proteins significantly enriched were a cellular response to pH, glycoprotein metabolic process, and other processes (Fig. 3B). Among the cellular components, the up-regulated DEPs were mostly derived from myofibril, actin cytoskeleton, actin cytoskeleton and sarcomere (Fig. 3C), while the down-regulated proteins were mainly concentrated in the glycoprotein metabolic process, preribosome, and Golgi-associated vesicle (Fig. 3D). The most prominent molecular functions mediated by the up-regulated DEPs were alpha-actinin binding, actin binding, cytoskeletal protein binding,

and GTPase activity (Fig. 3E). The down-regulated DEPs were enriched in molecular functions such as procollagen-proline dioxygenase activity, UDP-galactosyltransferase activity and oligosaccharyl transferase activity (Fig. 3F).

3.3.2.2. KEGG enrichment analysis. We also conducted KEGG enrichment analysis of the DEPs to identify signaling pathways. We found that on the whole, the significantly enriched pathways of the DEPs were the oxytocin signaling pathway, regulation of actin cytoskeleton, vascular smooth muscle contraction and focal adhesion (Fig. 4A). The up-regulated DEPs were mainly enriched in vascular smooth muscle contraction, the cGMP-PKG signaling pathway as well as focal adhesion (Fig. 4B). The down-regulated proteins were mostly enriched in protein export, other types of O-glycan biosynthesis, and various types of N-glycan biosynthesis (Fig. 4C).

3.4. PRM validation analysis

According to the mass spectrometry data of the LFQ, we selected 1–2 independent peptides for every protein to qualify PRM. We chose the DEPs with the lower *P*-value and higher fold change, and every DEP was a functional protein or transcription factor, excluding cytoskeletal protein. A total of 7 target proteins (PGM5, CAMK2G, ABHD6, MYLK, SYNPO2, IRAG1, and ADIPOQ) were identified, and the changes in validated proteins between adhesion and control groups are displayed in Fig. 5. The relative abundance and fold-change values of these proteins were notably increased, and functional analysis from proteomics revealed that they participated in significantly enriched classifications of GO and KEGG. Among them, Four proteins (including ADIPOQ, MYLK, CAMK2G, and SYNPO2) mainly played molecular functions of binding, of which the highest differential expression was MYLK with the Adhesion/Control ratio in PRM of 7.95. Three proteins (including SYNPO2, ABHD6, and MYLK) took part in the cell process of regulation of cell migration. Two proteins (including MYLK and IRAG1) were involved in the vascular smooth muscle contraction pathway. Another two proteins (including MYLK and CAMK2G) were involved in the cGMP-PKG and calcium signaling pathway. The PRM results were highly

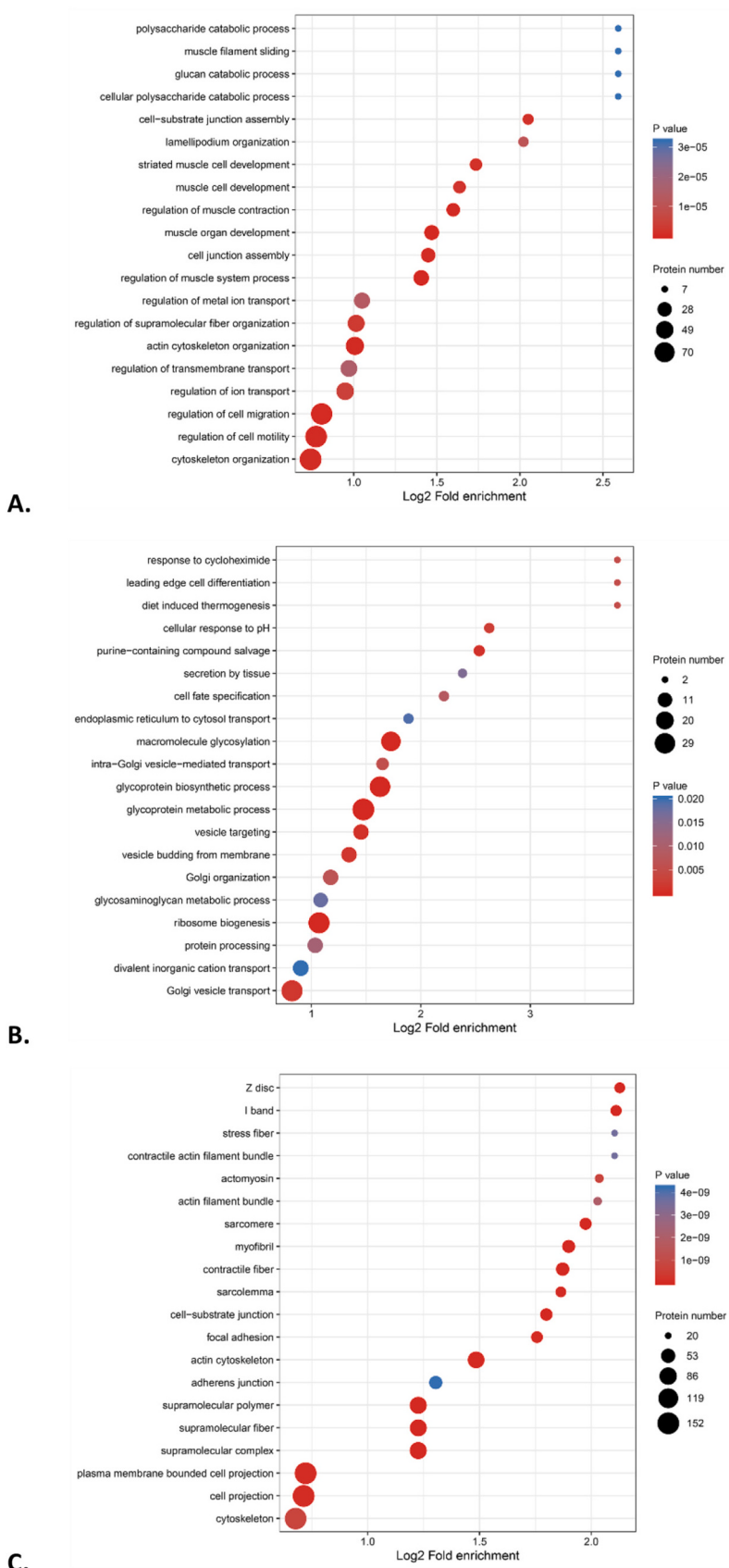


Fig. 3. Enrichment analysis for biological processes, cellular components, and molecular functions of the up-and down-regulated DEPs. The color of the circle indicated the *P* values of enrichment, while the circle size indicated the number of DEPs in the functional class.

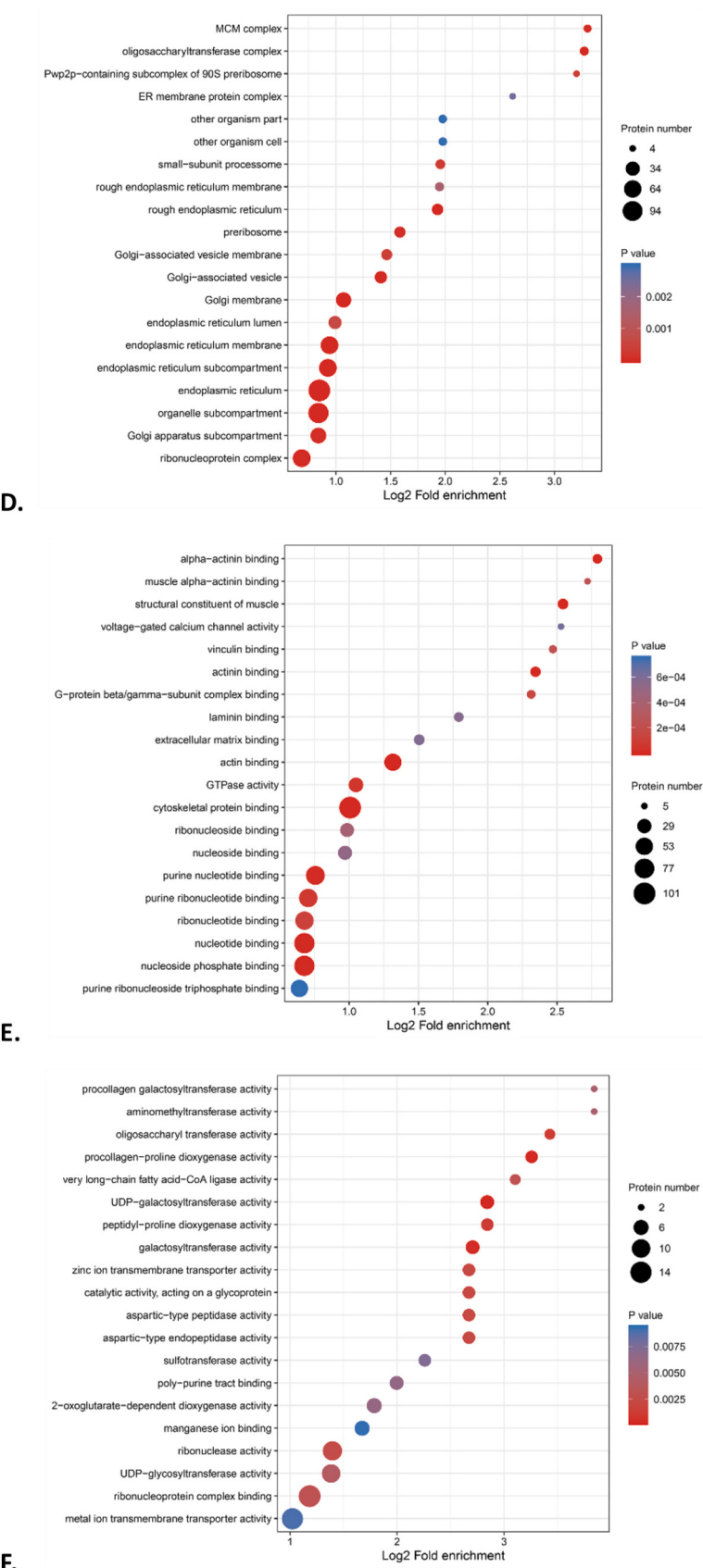


Fig. 3. (continued).

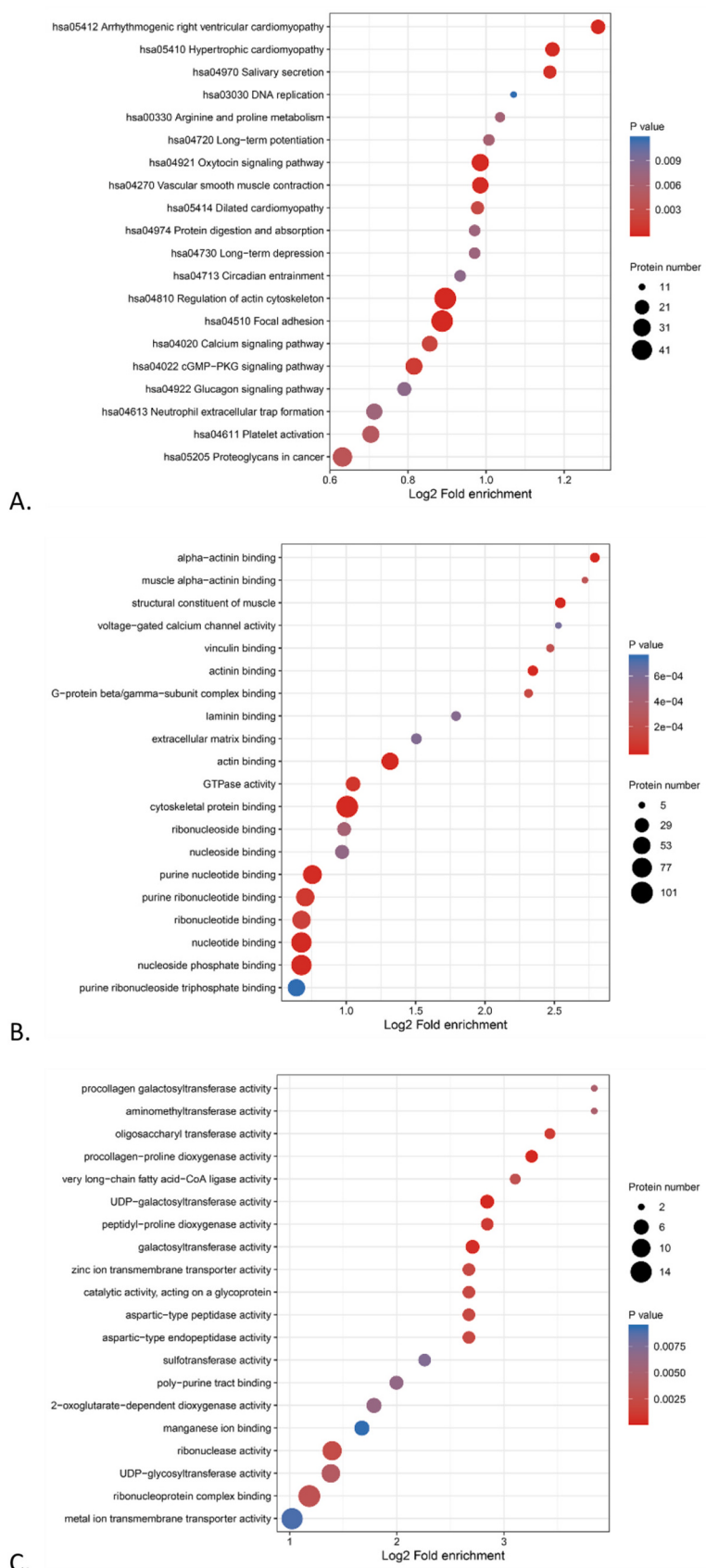


Fig. 4. The enrichment analysis of the DEPs between the IUA tissues and the control group. A, KEGG pathway enrichment analysis of all the DEPs. B, The KEGG-enriched pathways of the up-regulated DEPs. C, The KEGG pathway enrichment analysis of the down-regulated DEPs. The color of the circles indicated the significant *P* values of the enrichments, and the size of the circles indicated the number of the DEPs in the functional class or pathways.

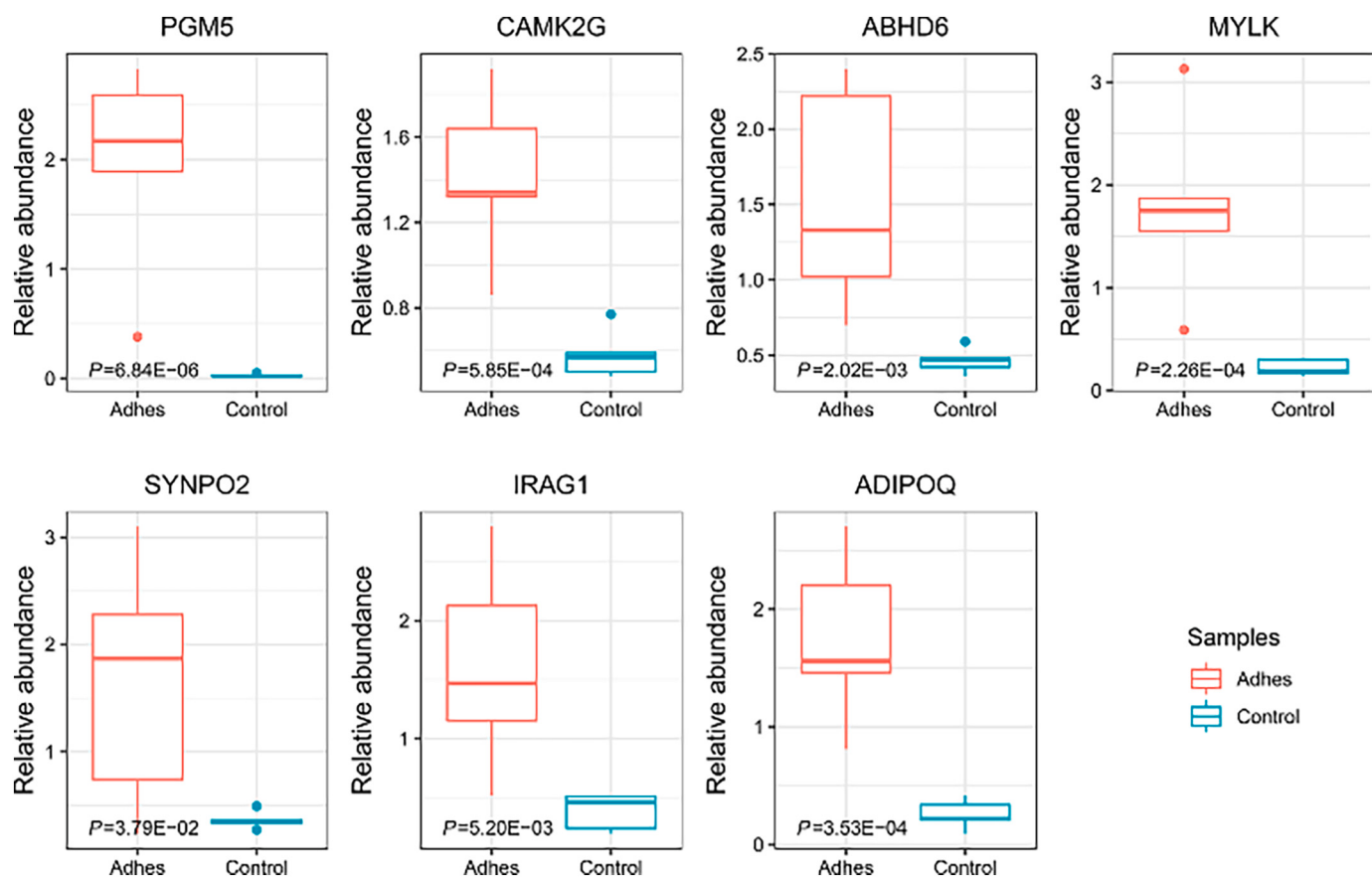


Fig. 5. The box plot of the 7 confirmed proteins in Adhesion groups and Control groups.

Table 2

The expression differences of the selected DEPs were verified by PRM.

Protein accession	Gene name	Protein description	Relative Abundance		Adhesion/Control Ratio In LFQ	Adhesion/Control Ratio in PRM	KEGG pathway
			Adhesion Average	Control Average			
Q15746	MYLK	Myosin light chain kinase, smooth muscle	2.394	0.302	13.06	7.95	hsa04510 Focal adhesion; hsa04810 Regulation of actin cytoskeleton; hsa04270 Vascular smooth muscle contraction; hsa04921 Oxytocin signaling pathway; hsa04020 Calcium signaling pathway; hsa04611 Platelet activation; hsa04371 Apelin signaling pathway; hsa04022 cGMP-PKG signaling pathway.
Q15124	PGM5	Phosphoglucomutase-like protein 5	2.92	0.04	16.767	73.19	
Q9BV23	ABHD6	Monoacylglycerol lipase ABHD6	1.708	0.518	14.539	3.29	hsa04723 Retrograde endocannabinoid signaling.
Q13555	CAMK2G	Calcium/calmodulin-dependent protein kinase type II subunit gamma	1.752	0.694	14.53	2.53	hsa04360 Axon guidance; hsa05200 Pathways in cancer; hsa04310 Wnt signaling pathway; hsa05205 Proteoglycans in cancer; hsa04012 ErbB signaling pathway; hsa05214 Glioma; hsa04020 Calcium signaling pathway; hsa04066 HIF-1 signaling pathway; hsa04722 Neurotrophin signaling pathway; hsa04921 Oxytocin signaling pathway; hsa04750 Inflammatory mediator regulation of TRP channels; hsa04024 cAMP signaling pathway; hsa04912 GnRH signaling pathway.
Q9UMS6	SYNPO2	Synaptopodin-2	2.126	0.464	4.648	4.59	
Q9Y6F6	IRAG1	Inositol 1,4,5-triphosphate receptor-associated 1	1.972	0.468	5.959	4.22	hsa04270 Vascular smooth muscle contraction; hsa04022 cGMP-PKG signaling pathway.
Q15848	ADIPOQ	Adiponectin	2.27	0.332	8.857	6.81	hsa03320 PPAR signaling pathway; hsa04920 Adipocytokine signaling pathway; hsa04152 AMPK signaling pathway.

in line with those of the label-free quantitative proteomics, and the data of these 7 proteins may be used as potential therapeutic targets. (Table 2).

4. Discussion

IUA is mainly secondary to the injury of the uterine cavity, such as curettage and intrauterine infection [10]. Many patients will suffer from postpartum complications of placental adhesions placenta accrete that affect physical and mental health [11]. At present, the mechanism of IUA needs further in-depth research, which can provide a theoretical basis for clinicians to identify pivotal molecules related to the pathogenesis and progression of the disease.

The majority of previous research has concentrated on transcriptomic analysis. Through the miRNA-gene network, 16 differentially expressed miRNAs regulated 54 target genes in the endometrium of severe IUA. The most significant target genes were miR-543 and CDH2 [12]. Zhang et al. [13] selected differentially expressed miRNAs and lncRNAs related to the IUA, such as ADIRF-AS1 and miR-326, and constructed the ceRNAs network. KEGG analysis indicated that numerous same KEGG paths were discovered between transcriptomic and proteomic analysis, such as vascular smooth muscle contraction, focal adhesion, and cGMP-PKG signaling pathway. But no clear reports have been made in proteomics.

We used label-free quantitative proteomics (LFQ) analysis to investigate the IUA-associated proteome for novel early diagnostic biomarkers. Through bioinformatics analysis, we found those DEPs are involved in KEGG pathways such as regulation of actin cytoskeleton, oxytocin signaling pathway and calcium signaling pathway are significantly enriched, which the pathways were different from transcriptomics. Subsequently, to determine the reliability of these proteins as new marker proteins, we selected 7 proteins with significant differences for PRM quantitative analysis, which further confirmed that they could be used as potential marker proteins. These proteins haven't been discovered previously in the research of the IUA. High expression of PGM5 can inhibit the proliferation, migration, and invasion of breast and colon cancer cells. Meanwhile, PGM5 can enhance the expression of epithelial marker E-cadherin, and the expression of mesenchymal marker vimentin is reduced, suggesting that PGM5 functions inhibit epithelial-mesenchymal transition [14,15]. As mentioned above, the nature of IUA is endometrial fibrosis with marked epithelial EMT occurring [16]. However, whether PGM5 is involved in the occurrence of EMT in IUA has not been reported. CAMKII γ is a multifunctional serine/threonine kinase that stimulates malignant cell proliferation and colony formation by upregulating the JAK2/Stat3 pathway and is required for multiple myeloma progression and poor clinical outcomes [17]. When MYLK expression is reduced in the inflammatory response, apoptosis is increased, leading to a decrease in smooth muscle cells and contractile dysfunction [18]. ABHD6 can inhibit the increase of pro-inflammatory factors such as IL-6 and IL-1 β in the body, thereby exerting an anti-inflammatory effect [19]. However, when ABHD6 is over-expressed in vivo, it can aggravate the growth and invasiveness of small cell lung cancer [20]. Liu et al. [21] found that down-regulation of SYNPO2 can activate YAP/TAZ signaling, exacerbating the invasive process of breast cancer cells in early metastasis and late colonization in the human body. When IRAG1 is deficient in the body, gastrointestinal dysfunction may occur, causing gastrointestinal bleeding, which in turn leads to anemia and splenomegaly [22]. As an adipose tissue-derived hormone, adiponectin has powerful anti-inflammatory and anti-fibrotic effects [23,24]. It can reduce inflammation and fibrosis in keloids by downregulating the expression of the signaling molecule CTGF downstream of the TGF- β 1/Smad pathway and activating the AMPK pathway formation [25,26].

As can be seen that the target protein mostly plays a role in fibrosis and cancer cell proliferation. Although our study screened and verified the target protein of IUA, the sample size of the research was small. In

the future, we will increase the accuracy of the experiment by expanding the sample size. In addition, alternative quantitative detection methods such as Western blotting and ELISA can be used to verify the target protein. Before these biomarkers are used as targets for clinical treatment of IUA, we will collect more reliable specimens to verify the characteristics of target proteins and related pathways, and strive to provide a new perspective for future research.

5. Conclusion

In summary, we constructed a proteomic map for the first time between IUA tissues and normal endometrial tissues by label-free quantitative proteomic analysis. We identified 1328 DEPs in total. Based on functional analysis and further PRM verification, 7 target proteins were obtained. These proteins may become the candidate therapeutic target of IUA, which may provide molecular evidence for IUA research and deepen our understanding of the pathological mechanism of the IUA.

Authors contributions

LY and KC conceived and designed the study. YJ, LH and RY prepared the materials involved in this study. LY took part in the experimental design. LY and YJ analyzed the data and drafted the manuscript. The manuscript was read and approved by all the authors.

Funding

This research was supported by Key Class B Project of Jiangsu Provincial Health Commission (grant number: ZDB2020031) and Jiangsu Province Maternal and Child Health Gynecological Medicine Project (grant number: F202006).

Declaration of Competing Interest

The authors declare that they have no conflict of interest.

Data availability

Data will be made available on request.

Acknowledgments

We thank Jingjie PTM BioLab(Hangzhou) Co., Ltd. and all the other members of the plant virology laboratory at Yangzhou University for their helpful suggestions and constructive criticism.

Appendix A. Supplementary data

Supplementary data to this article can be found online at <https://doi.org/10.1016/j.jprot.2023.104854>.

References

- [1] B. Li, Q. Zhang, J. Sun, D. Lai, Human amniotic epithelial cells improve fertility in an intrauterine adhesion mouse model, *Stem Cell Res Ther* 10 (1) (2019) 257. Published 2019 Aug 14, <https://doi.org/10.1186/s13287-019-1368-9>.
- [2] C.A. Salazar, K. Isaacson, S. Morris, A comprehensive review of Asherman's syndrome: causes, symptoms and treatment options, *Curr. Opin. Obstet. Gynecol.* 29 (4) (2017) 249–256, <https://doi.org/10.1097/GCO.0000000000000378>.
- [3] L. Liu, G. Chen, T. Chen, et al., si-SNHG5-FOXF2 inhibits TGF- β 1-induced fibrosis in human primary endometrial stromal cells by the Wnt/ β -catenin signalling pathway, *Stem Cell Res Ther* 11 (1) (2020) 479. Published 2020 Nov 11, <https://doi.org/10.1186/s13287-020-01990-3>.
- [4] D. Yu, Y.M. Wong, Y. Cheong, E. Xia, T.C. Li, Asherman syndrome—one century later, *Fertil. Steril.* 89 (4) (2008) 759–779, <https://doi.org/10.1016/j.fertnstert.2008.02.096>.
- [5] A. Abdukeyoumu, M.Q. Li, F. Xie, Transforming growth factor- β 1 in intrauterine adhesion, *Am. J. Reprod. Immunol.* 84 (2) (2020), e13262, <https://doi.org/10.1111/aji.13262>.

- [6] C. Li, W. Wang, S. Sun, Y. Xu, Z. Fang, L. Cong, Expression and potential role of MMP-9 in intrauterine adhesion, *Mediat. Inflamm.* (2021), <https://doi.org/10.1155/2021/6676510>, 2021:6676510. Published 2021 Jan 29.
- [7] N.N. Bi, S. Zhao, J.F. Zhang, et al., Proteomics investigations of potential protein biomarkers in sera of rabbits infected with *Schistosoma japonicum*, *Front. Cell. Infect. Microbiol.* 11 (2021), 784279. Published 2021 Dec 22, <https://doi.org/10.3389/fcimb.2021.784279>.
- [8] S. Tyanova, T. Temu, J. Cox, The MaxQuant computational platform for mass spectrometry-based shotgun proteomics, *Nat. Protoc.* 11 (12) (2016) 2301–2319, <https://doi.org/10.1038/nprot.2016.136>.
- [9] The Gene Ontology Consortium, The gene ontology resource: 20 years and still GOing strong, *Nucleic Acids Res.* 47 (D1) (2019) D330–D338, <https://doi.org/10.1093/nar/gky1055>.
- [10] R. Azizi, L. Aghebati-Maleki, M. Nouri, F. Marofi, S. Negargar, M. Yousefi, Stem cell therapy in Asherman syndrome and thin endometrium: stem cell- based therapy, *Biomed. Pharmacother.* 102 (2018) 333–343, <https://doi.org/10.1016/j.biopha.2018.03.091>.
- [11] J. Du, H. Lu, X. Yu, et al., The effect of icariin for infertile women with thin endometrium: a protocol for systematic review, *Medicine (Baltimore)* 99 (12) (2020), e19111, <https://doi.org/10.1097/MD.00000000000019111>.
- [12] X. Liu, H. Duan, H.H. Zhang, L. Gan, Q. Xu, Integrated data set of microRNAs and mRNAs involved in severe intrauterine adhesion, *Reprod. Sci.* 23 (10) (2016) 1340–1347, <https://doi.org/10.1177/1933719116638177>.
- [13] J. Zhang, P. Jiang, Y. Tu, et al., Identification and validation of long non-coding RNA associated ceRNAs in intrauterine adhesion, *Bioengineered.* 13 (1) (2022) 1039–1048, <https://doi.org/10.1080/21655979.2021.2017578>.
- [14] Y. Sun, H. Long, L. Sun, et al., PGM5 is a promising biomarker and may predict the prognosis of colorectal cancer patients, *Cancer Cell Int.* 19 (2019) 253. Published 2019 Oct 1, <https://doi.org/10.1186/s12935-019-0967-y>.
- [15] F. Ran, Y. Zhang, Y. Shi, et al., miR-1224-3p PROMOTES breast cancer cell proliferation and migration through PGM5-mediated aerobic glycolysis, *J. Oncol.* (2021), <https://doi.org/10.1155/2021/5529770>, 2021:5529770. Published 2021 Apr 19.
- [16] G. Zhao, R. Li, Y. Cao, et al., ΔNp63 α -induced DUSP4/GSK3 β /SNAI1 pathway in epithelial cells drives endometrial fibrosis, *Cell Death Dis.* 11 (6) (2020) 449. Published 2020 Jun 11, <https://doi.org/10.1038/s41419-020-2666-y>.
- [17] L. Yang, B. Wu, Z. Wu, et al., CAMKII γ is a targetable driver of multiple myeloma through CaMKII γ / Stat3 axis, *Aging (Albany NY)* 12 (13) (2020) 13668–13683, <https://doi.org/10.18632/aging.103490>.
- [18] Y. Song, P. Liu, Z. Li, et al., The effect of myosin light chain kinase on the occurrence and development of intracranial aneurysm, *Front. Cell. Neurosci.* 12 (2018) 416. Published 2018 Nov 13, <https://doi.org/10.3389/fncel.2018.00416>.
- [19] M. Alhouayek, J. Masquelier, P.D. Cani, D.M. Lambert, G.G. Muccioli, Implication of the anti-inflammatory bioactive lipid prostaglandin D2-glycerol ester in the control of macrophage activation and inflammation by ABHD6, *Proc. Natl. Acad. Sci. U. S. A.* 110 (43) (2013) 17558–17563, <https://doi.org/10.1073/pnas.1314017110>.
- [20] Z. Tang, H. Xie, C. Heier, et al., Enhanced monoacylglycerol lipolysis by ABHD6 promotes NSCLC pathogenesis, *EBioMedicine.* 53 (2020), 102696, <https://doi.org/10.1016/j.ebiom.2020.102696>.
- [21] J. Liu, L. Ye, Q. Li, et al., Synaptotagmin-2 suppresses metastasis of triple-negative breast cancer via inhibition of YAP/TAZ activity, *J. Pathol.* 244 (1) (2018) 71–83, <https://doi.org/10.1002/path.4995>.
- [22] M. Majer, S. Prueschenk, J. Schlossmann, Loss of PKG β /IRAG1 signaling causes anemia-associated splenomegaly, *Int. J. Mol. Sci.* 22 (11) (2021) 5458. Published 2021 May 21, <https://doi.org/10.3390/ijms22115458>.
- [23] F. Fang, L. Liu, Y. Yang, et al., The adipokine adiponectin has potent anti-fibrotic effects mediated via adenosine monophosphate-activated protein kinase: novel target for fibrosis therapy, *Arthritis Res Ther.* 14 (5) (2012) R229. Published 2012 Oct 23, <https://doi.org/10.1186/ar4070>.
- [24] H. Jing, S. Tang, S. Lin, et al., Adiponectin in renal fibrosis, *Aging (Albany NY)* 12 (5) (2020) 4660–4672, <https://doi.org/10.18632/aging.102811>.
- [25] L. Luo, J. Li, H. Liu, et al., Adiponectin is involved in connective tissue growth factor-induced proliferation, migration and overproduction of the extracellular matrix in keloid fibroblasts, *Int. J. Mol. Sci.* 18 (5) (2017) 1044. Published 2017 May 12, <https://doi.org/10.3390/ijms18051044>.
- [26] L. Luo, J. Li, Y. Wu, J. Qiao, H. Fang, Adiponectin, but not TGF- β 1, CTGF, IL-6 or TNF- α , may be a potential anti-inflammation and anti-fibrosis factor in keloid, *J. Inflamm. Res.* 14 (2021) 907–916. Published 2021 Mar 16, <https://doi.org/10.2147/JIR.S301971>.